

**CFD SIMULATIONS OF ANNULAR DISTRIBUTOR OF
SWIRLING FLUIDIZED BED (SFB) REACTOR**

By

Syaida Hazira Binti Ramli

A project dissertation submitted to the

Mechanical Engineering Programme

Universiti Teknologi PETRONAS

in partial fulfilment of the requirement for the

BACHELOR OF ENGINEERING (Hons)

(MECHANICAL ENGINEERING)

JANUARY 2012

Universiti Teknologi PETRONAS

Bandar Seri Iskandar

31750 Tronoh

Perak Darul Ridzuan

CERTIFICATION OF APPROVAL

CFD SIMULATIONS OF ANNULAR DISTRIBUTOR OF

SWIRLING FLUIDIZED BED (SFB) REACTOR

By

Syaida Hazira Binti Ramli

A project dissertation submitted to the
Mechanical Engineering Programme
Universiti Teknologi PETRONAS
in partial fulfilment of the requirement for the
BACHELOR OF ENGINEERING (Hons)
(MECHANICAL ENGINEERING)

Approved by,

(Prof Vijay R. Raghavan)

UNIVERSITI TEKNOLOGI PETRONAS
TRONOH, PERAK
January 2012

CERTIFICATION OF ORIGINALITY

This is to certify that I am responsible for the work submitted in this project, that the original work is my own except as specified in the references and acknowledgements, and that the original work contained herein have not been undertaken or done by unspecified sources or persons.

(SYAIDA HAZIRA BINTI RAMLI)

MECHANICAL ENGINEERING

UNIVERSITI TEKNOLOGI PETRONAS

ABSTRACT

This work reports the findings of CFD simulations on a swirling fluidized bed which operates with an annular distributor. The simulations were carried out to predict the pressure and velocity distribution when the fluidizing gas/ air flows through the passage between the trapezoidal blades of the annular distributor. It is normally assumed that the air flow characteristic through the distributor is affected by various aspects of the distributor like blade overlaps, blade inclinations etc. Flow characteristics in the distributor provide us with the fundamental understanding of the bed behaviour along with ideas for further improvement in the fluidization quality hence needed to be studied in detail. Thus, the current study was carried out to investigate the flow characteristics and predict non-uniformity in flow through the annular distributor of a swirling fluidized bed. Inappropriate blade configurations will lead to an unsatisfactory fluidization and mixing of the air and bed particles.

In this project, a commercial CFD package, FLUENT 6.3, was used to simulate the flow through the annular distributor. The velocity and pressure profiles for various blade designs were investigated in order to lead to an understanding of the flow and the particle mixing behaviour inside the reactor. The objective of this project is to obtain the pressure and velocity profiles at the distributor outlet based on various operating variables including air inlet velocities, blade overlap angles (9° , 12° , 15° , and 18°), blade inclinations (10° and 15°), along with variations in the opening between the distributor blades. The most significance finding of this work is that the fluid tend to flow through a path with least resistance which is having a largest cross section area and shortest path length. The dynamic characteristic obtained from CFD simulations have been validated with experimental results and a good agreement has been observed.

ACKNOWLEDGEMENT

First and foremost, I would like to express my praises to GOD for His blessing.

My deepest appreciation and gratitude is extended to my supervisor, Prof Vijay R. Raghavan for the continuous support of my final year project, for his patience, motivation, enthusiasm, and immense knowledge. His guidance helped me in all the time of research and writing of this thesis.

Also to my co- supervisor, Mr. Vinod Kumar, thank you for readily providing me with the necessary information required to conduct the project and clarifications whenever I needed them. I also wish to thank other lecturers and staff of Mechanical Engineering Department, Universiti Teknologi Petronas for their cooperation, suggestions and guidance in the compilation and preparation this final year project thesis.

Deepest thanks and appreciation to my parents, family, and others for their cooperation, encouragement, constructive suggestions and full support for the thesis completion, from the beginning till the end. Also thanks to all of my friends and everyone, who have contributed by supporting my work and help me during the final year project progress till it is fully completed.

.

TABLE OF CONTENTS

CERTIFICATION OF APPROVAL	ii
CERTIFICATION OF ORIGINALITY	iii
ABSTRACT	iv
ACKNOWLEDGEMENT	v
LIST OF TABLES	vii
LIST OF FIGURES	vii
CHAPTER 1	1
1.1 INTRODUCTION	1
1.2 PROBLEM STATEMENT	2
1.3 OBJECTIVES OF THE STUDY	5
1.4 SCOPE OF STUDY	5
1.5 RELEVANCY OF STUDY	5
CHAPTER 2	6
LITERATURE REVIEW	6
CHAPTER 3	9
METHODOLOGY	9
CHAPTER 4	13
RESULTS AND DISCUSSION	13
CHAPTER 5	22
CONCLUSIONS AND RECOMMENDATION	22
CHAPTER 6	23
REFERENCES	23
CHAPTER 7	25
APPENDICES	25

LIST OF TABLES

Table 1: Simplest case for 1-D divergent blade passage.....	13
Table 2 : Analysis of SFB blade for 128 different cases.....	14
Table 3 : Velocity and pressure profile for 9 degree overlap angle with 15° inclination angle ...	17
Table 4 : Velocity and pressure profile for 9 degree overlap angle with 20° inclination angle ...	18
Table 5 : Velocity and pressure profile for 12 degree overlap angle with 15° inclination angle..	19
Table 6 : Velocity and pressure profile for 12 degree overlap angle with 20° inclination angle..	20

LIST OF FIGURES

Figure 1 : Detail view of Swirling fluidized bed with enlarged annular blade distributor.....	2
Figure 2 : 1-Directional divergent flow with varying cross-section.....	3
Figure 3: 1-D divergent flow with varying path length	3
Figure 4 : Fundamental study of flow development in 2 different cases	4
Figure 5: Parameters required for blade design.....	9
Figure 6: Geometry modelled in CATIA	10
Figure 7: Meshing and boundary condition applied in GAMBIT	10
Figure 8: Contour and vector display	11
Figure 9: Summary of methodology for the whole simulation process	12
Figure 10 : Drafting of blade showing all the parameters for calculation.	15
Figure 11 : Flow pattern and flow development in 2-D divergent blade passage	21

CHAPTER 1

1.1 INTRODUCTION

Fluidized bed reactor

A fluidized bed reactor (FBR) can be used to carry out a variety of multiphase processes. In this type of reactors, a fluid (gas or liquid) is passed through bed of solids (such as catalyst particle) at velocities high enough to create fluidization. Because of its merits; the fluidized bed reactor is now used in many industrial applications.

In a packed bed reactor, as the fluid velocity is increased, the reactor will reach a stage where the force of the fluid on the solids is enough to balance the weight of the solid material. This stage is known as incipient fluidization and occurs at this minimum fluidization velocity. Once this minimum velocity is surpassed, the contents of the reactor bed begin to expand and swirl around much like an agitated tank or boiling pot of water. The reactor is now a fluidized bed. Depending on the operating conditions and properties of solid phase, various flow regimes can be observed in this reactor.

The swirling fluidized bed is one of recent variants in fluidized bed operation. Contrary to the conventional fluidization, the fluid (gas) enters the bed at an inclined angle to the horizontal. It is directed by a suitable design of distributor which is now designated as annular distributor. The annular distributor used in swirling fluidized bed imparts special characteristics to the bed which are considerably different from that of the conventional fluidized bed.

Computational fluid dynamics (CFD) can play a key role in helping to understand the flow within the distributor. CFD has been used in the last two decades to devise solutions and gain insight of the flow inside the mixing tank and CFD, together with experimental validation, has been able to improve the design of many reactor systems. The focus of this project is to predict the mixing behaviour inside the reactor and to investigate the effect of blade design, velocity and pressure on the flow characteristics. The process was simulated based on the literature with the blade design data by several articles and its results were to be compared as a validation to the simulation data. The good comparison indicates the validity of the CFD model.

1.2 PROBLEM STATEMENT

In the set of blades in SFB, the flow diverges in two directions which is in y and z directions. The path length varies along the Y direction, while the cross sectional area (i.e., flow area) between 2 blades, normal to the z-direction, also varies. Figures below show the picture of a swirling fluidized bed with the enlarged annular distributor.

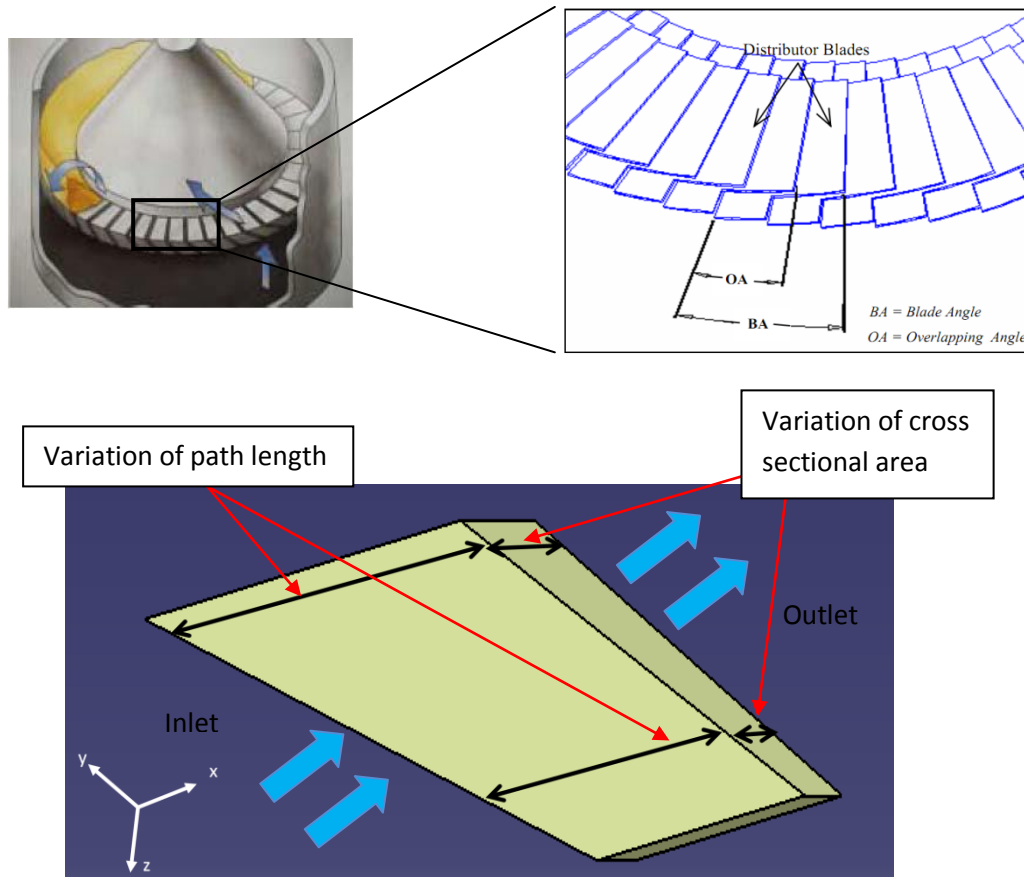


Figure 1 : Detail view of Swirling fluidized bed with enlarged annular blade distributor.

In order to study the complex flow characteristic used in the SFB shown above, simpler cases have been studied and simulated which are 1-D divergence of variation in cross section area and 1-D divergence variation in path length. In the case of flow with 1-D divergence of variation in cross-section area, the largest cross section provides least flow resistance as shown in Fig.2. As a result, the following velocity contour was obtained, with most of the flow concentrated at the largest cross-section area at the outlet, as anticipated.

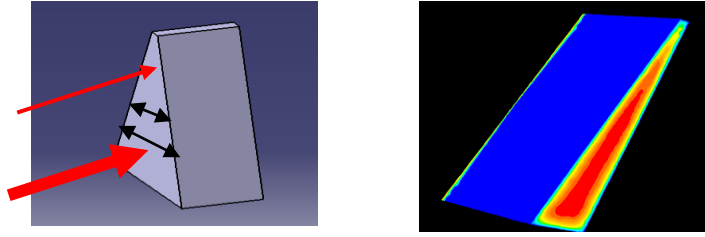


Figure 2 : 1-Directional divergent flow with varying cross-section

For the second case of 1-D divergent flow with varying path length, the shortest path provides least resistance to flow. As a result, the following contour was obtained with most of the flow concentrated at the shortest path at the outlet.

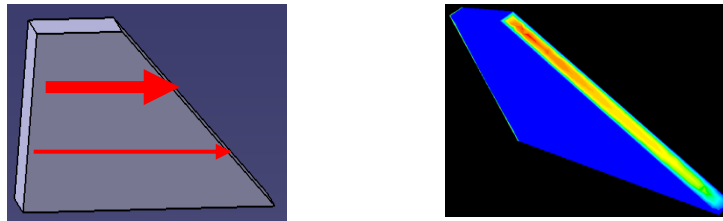


Figure 3: 1-D divergent flow with varying path length

In both figure 2 and figure 3, the thickness of the flow coloured arrow indicating the relative magnitude of the flow.

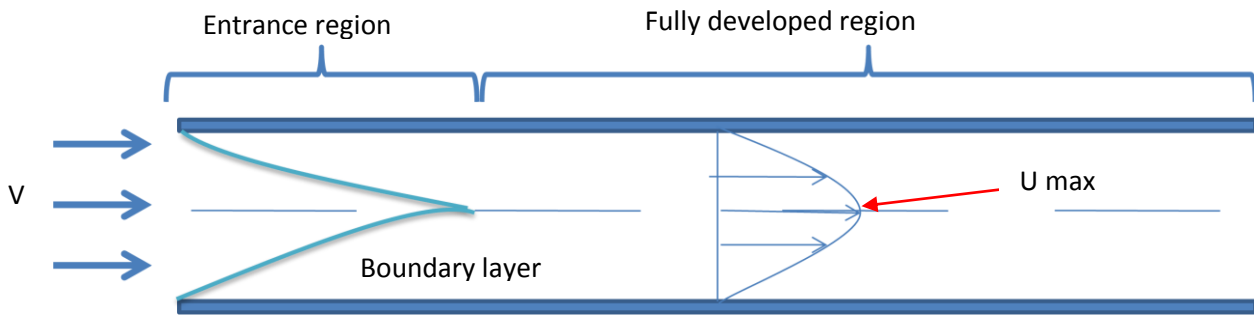
However, flow with combination of both factors of variation in cross section areas and path lengths (termed as 2-D divergence) for blade used in SFB (refer figure 1) have been currently studied to discover the major determinant in fluid flow. The smallest cross section area (high resistance) is compensated with shortest path (low resistance). Similarly, the longest path length (high resistance) is compensated with largest flow area (low resistance). It is impossible to determine, a priori, what flow path will be predominant. However, it can be expected that the flow will not be uniform.

Therefore, the problem to determine how the flow would occur in a trapezoidal passage with 2-D directional divergence is an interesting question in fluid flow. Further, if the two planes are inclined so that the boundary layers do not develop simultaneously, it is an interesting question as to what the flow would be like.

The answers to these questions are of fundamental importance in Fluid Mechanics. They are also important in an application such as the blade space in the annular distributor of a Swirling Fluidized Bed.

Fundamental study of flow development in simple cases.

Case 1 : Flow development in long parallel plate



Case 2 : Flow development in short parallel plate



Figure 4 : Fundamental study of flow development in 2 different cases

The velocity of flow in boundary layer increases from zero at the surface to free stream velocity at the edge of the boundary layer. Velocity gradient exists only at the boundary layer.

In long parallel plate, at some distance from the entrance, the boundary layers merge up to a point and the velocity profile beyond this point remains unchanged (fully developed).

While in a short parallel plate, the boundary layer will not be fully develop due to a very short distance. However, the velocity at core region is higher compared to the fluid velocity entering the passage. Therefore, the flow is said to be asymmetric undeveloped flow with the accelerating velocity at the center.

1.3 OBJECTIVES OF THE STUDY

The objective of this project is to obtain the pressure and velocity variation at the distributor outlet of 2-D divergent trapezoidal blade passage based on various operating variables including air inlet velocity, geometry of cross-section, blade length and blade width. This work also aims to get the flow variation if the blade opening is inclined.

1.4 SCOPE OF STUDY

This study is limited to the simulation of:-

- 1) trapezoidal blade with 2-D divergent of various cross section and blade length
- 2) blade opening inclined at different angle (15° to 20°)
- 3) range of blade gaps (1mm to 3 mm)
- 4) Inlet velocity applied at the blade opening ranging from 0.1m/s to 3.5 m/s

1.5 RELEVANCY OF STUDY

The significance of this study is to identify characteristics of flow distributions in a swirling fluidized bed gas distributor. Although the available distributors have been used and show good performance, this study is necessary to investigate what are the other factors related to the distributor design that can produce good uniformity and further improve fluidized bed performance. This study aims to identify the major determinant (either varying cross section or varying blade length) that will cause the fluid to flow through the blade passage from inlet to the outlet of the distributor. Results from this study can be used for designing a better distributor for swirling fluidized bed.

CHAPTER 2

LITERATURE REVIEW

1. Flow development in close conduit

Many researchers had come out with various results to study the flow development in a close conduit with different shapes of cross section. Damean and Regtien [1] encountered the design process of the hexagonal ducts etched in $\langle 100 \rangle$ silicon, namely, the achievement of the Poiseuille number Po for the velocity field of the fully developed laminar flow. They developed a procedure for obtaining Po versus the aspect ratio of the hexagonal cross section. The validity of this procedure is proven using different shapes of cross sections. They underline the merit of this procedure, namely, its applicability using a commercial software package.

Thomas, Richard, and Yerkes [2] analyze the behavior of liquid flowing in a groove with a trapezoidal cross-section. For fully developed laminar flow, the conservation of mass and momentum equations reduce to the classic Poisson equation in terms of the liquid velocity. A finite difference solution was employed to determine the mean velocity, volumetric flow rate, and Poiseuille number ($Po=fRe$) as functions of the groove aspect ratio, groove-half angle, meniscus contact angle and imposed shear stress at the liquid–vapor interface.

Experiment was conducted by Husain and Kwang [3] on a microchannel heat sink shape optimization using response surface approximation. Three design variables related to microchannel width, depth, and fin width are selected for optimization, and thermal resistance has been taken as objective function. Design points are chosen through a three-level fractional factorial design of sampling methods. Navier–Stokes and energy equations for steady, incompressible, and laminar flow and conjugate heat transfer are solved at these design points using a finite volume solver. Solutions are carefully validated with the analytical and experimental results.

Currently, McHale and Garimella [4] investigated Heat transfer in the thermal entrance region of trapezoidal microchannels for hydrodynamically fully developed, single-phase, laminar flow with no-slip conditions. Three-dimensional numerical simulations were performed using a finite-volume approach for trapezoidal channels with a wide range of aspect ratios. The sidewall angles of 54.7° and 45° are chosen to correspond to etch-resistant planes in the crystal structure of silicon. Local and average Nusselt numbers are reported as a

function of dimensionless length and aspect ratio. The effect of Prandtl number upon the thermal entrance condition is explored. The fully developed friction factors are computed and correlated as a function of channel aspect ratio.

Huzayyin and Manglik [5] obtained a Computational solutions by second-order accurate control-volume schemes, highlighting the effects of geometry and thermal condition on the Nusselt numbers (Nu_T and Nu_{HI}), and the results complement and extend the literature on compact-channel internal forced convection. Also, as a design and optimization tool for the practicing engineer, polynomial functions of the flow cross section aspect ratio are presented to predict both the friction factor and the Nusselt number for the different trapezoidal and triangular fin core geometries considered.

In extending the previous study, they also come up with a parametric study of the effect of the two dimensional duct geometry, which has symmetric fin wall corrugations of trapezoidal profile. The Reynolds Number range covered is between $10 < Re < 1000$ for air ($Pr = 0.72$) flows. The geometric variables are described by the divergent-plane's inclination angle Φ and the convergent-divergent amplitude ratio α . The wall perforations are modelled as uniformly distributed equi-size thin slots so as to render a porosity (ratio of perforated area to total surface area) β of 10% on the fin surface. The fin-wall transpiration (fluid injection in the divergent section and fluid suction in the convergent section) is seen to promote enhanced convective heat transfer by inducing cross stream mixing and periodic disruption of the boundary layer. As a result, increase in heat transfer is accompanied with a reduction in frictional loss.[6]

K. Dutkowski [12] has conducted an experimental investigation of pressure drop in minichannels, with use of water and air as the working fluids. The test section was made from stainless steel pipes with internal diameters of 0.55, 0.64 and 1.10 mm, respectively. A pressure drop was presented per a length unit as the function of Reynolds number. A comparison of the experimental friction factor with the results obtained from theoretical equations of Hagen–Poiseuille was presented. The experiments were conducted in range of Reynolds number $Re = 30$ up to transition to the turbulent flow.

Another experimental investigation on Reynold number is conducted by M. Akbari, D. Sinton and M. Bahrami [13] to verify the present model. 5 sets of rectangular microchannels with converging–diverging linear wall profiles that are fabricated and tested.

The study was to approximate model for determining the pressure drop of laminar, single-phase flow in slowly-varying microchannels of arbitrary cross-section based on the solution of a channel of elliptical cross-section. A new nondimensional parameter is introduced as a criterion to identify the significance of frictional and inertial effects. This criterion is a function of the Reynolds number and geometrical parameters of the cross-section; i.e., perimeter, area, cross-sectional polar moment of inertia, and channel length. It is shown that for the general case of arbitrary cross-section, the cross-sectional perimeter is a more suitable length scale.. The collected pressure drop data are shown to be in good agreement with the proposed model. Furthermore, the presented model is compared with the numerical and experimental data available in the literature for a hyperbolic contraction with rectangular cross-section.

Simultaneously developing velocity and temperature fields in the slip-flow regime are investigated numerically in trapezoidal microchannels with constant wall temperatures. A wide range of channel aspect ratios ($0.25 \leq \alpha \leq 2$) and side angles ($30^\circ \leq \phi \leq 90^\circ$) are considered in the Reynolds number range $0.1 \leq Re \leq 10$. A control-volume based numerical method is used to solve the Navier–Stokes and energy equations with velocity-slip and temperature-jump at the walls. As characterized by the Knudsen number ($Kn \leq 0.1$), the effects of rarefaction on the key flow features are examined in detail. The results show that the heat transfer coefficient is decreases strongly with increasing rarefaction and aspect ratio. However, as the aspect ratio increases, its sensitivity to Kn decreases. Practical engineering correlations are also provided for fully developed flow friction and heat transfer coefficients.[14]

2. *Fluidized bed*

Heat and mass transfer problems that arise in the design and operation of fluidized beds continue to receive substantial attention. Theoretical studies have been published on radiative heat transfer within gas fluidized beds and bed-to-wall radiative transport. Non-Newtonian effects and circulation in the fluid phase were the subjects of analysis. Experiments were reported on bed-to-wall heat transfer, particle motion and effects of particle properties. Some work on spray granulation and heat transfer to a single rising bubble has also appeared. [7]

CHAPTER 3

METHODOLOGY

The whole process requires a well-planned methodology in order to achieve the required objective. The methodology applied can be divided into 3 main parts which are pre-processing, preparation for solving and post-processing.

1. PRE-PROCESSING

Design of geometry in CATIA

Pre-processing stage involves preparing blade geometry using CATIA software with different parameters including blade inclinations, blade gaps and blade overlaps as shown in the figure below.

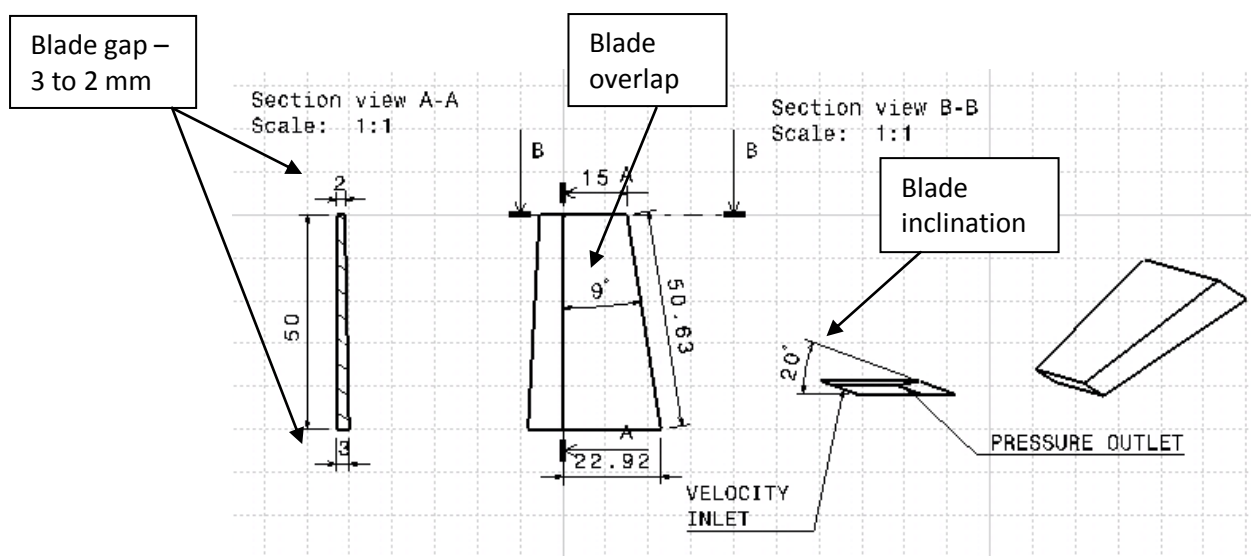


Figure 5: Parameters required for blade design.

Flow characteristics are required to be predicted inside the annular distributor for four sizes of blades known as blade overlaps. The blades resemble the shape of truncated sectors of a circle, having angles of $[9^\circ, 12^\circ, 15^\circ \text{ and } 18^\circ]$ respectively. The overlapping length between two successive blades helps to direct the air at the designated angle. Larger overlapping lengths of blades may result in higher distributor pressure drop. This is because larger overlapping lengths constrain the flow of air much longer between the blades before it enters the bed. For each size of blade, two degree blade inclinations had been considered $[15^\circ \text{ and } 20^\circ]$. Two blade gaps (3mm and 2mm as shown in figure above) and (2mm and 1mm) are

applied for each blade inclination. Then, both normal condition and symmetry condition are applied to all blade designs. Therefore, a total of 32 versions of blades with different geometries had been designed. The figure below is the isometric view of one of the blade geometries with 9° blade overlapping, 20° inclination and a blade gap of 2mm to 3mm at outer and inner radius respectively.

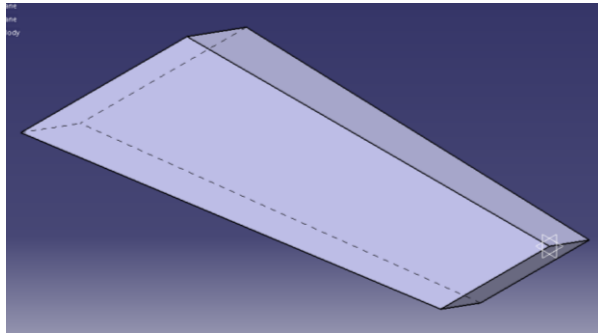


Figure 6: Geometry modelled in CATIA

The file is then saved as an .igs file so that it can be read in GAMBIT software for meshing purposes. Meshing is the discretization of a domain into smaller sub-domains in order to analyze the fluid flow since the partial differential equations that govern fluid flow and heat transfer are not usually amenable to analytical solutions, except for very simple cases. The meshing process started with edge meshing, face meshing in 2D element and followed by volume meshing in 3D element using quadrilateral mesh.

The meshed geometry is then applied with boundary conditions at its inlet, outlet and wall. Velocity and pressure are set at the inlet and outlet respectively. Then, the software will identify a wall condition to other faces as default. Material is assigned as air to the model. Figure below shows one of the meshed parts.

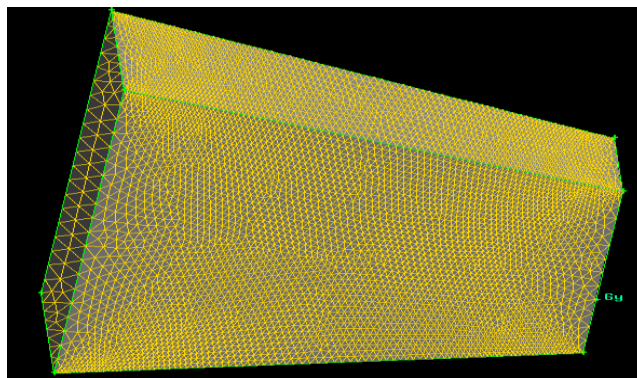


Figure 7: Meshing and boundary condition applied in GAMBIT

2. PREPARATION FOR SOLVING

Then, the meshed part is converted into .mesh file (.msh) to be read in FLUENT software. Once the geometry is imported, the grid checking is done where it will list the minimum and maximum x, y and z values from the grid in the default SI unit of meters, and will report a number of other grid features that are checked. Any errors in the grid will be reported at this time. Particularly, it is ensured that the minimum volume has to always be non-negative since FLUENT cannot begin a calculation when this is the case. The next step followed by grid scaling in order to set a unit to be mm (in this case) as the working unit for the whole process onwards.

Defining the model

Define the model solver, viscosity (laminar for normal condition and k-epsilon for the existence of turbulent flow), defining energy equation, materials (air in this case) and boundary condition comprising of velocity inlet, pressure outlet and wall. In the first boundary condition for velocity inlet, the first velocity applied is 1.7m/s followed by 2.5m/s, 3.0m/s and 3.5m/s for a particular geometry

3. POST-PROCESSING

This is the final step in CFD analysis, and it involves the results and interpretation of the predicted flow data. The main outcomes of post-processing are domain geometry and grid display, contour plot, vector plots, 2D surface plots, x-y plot with different properties and plot convergence.

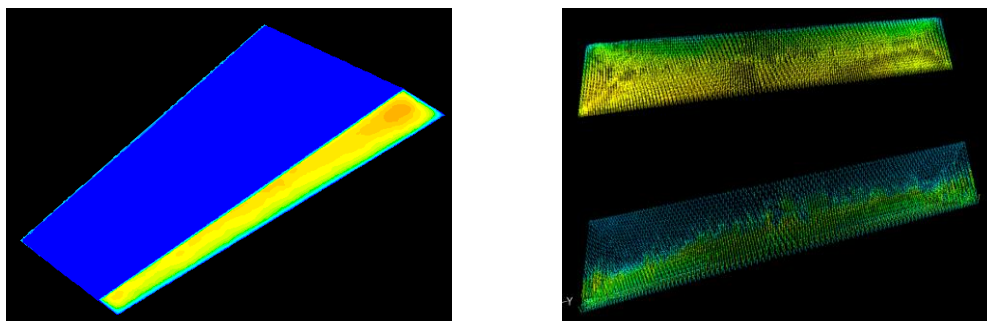


Figure 8: Contour and vector display



- Model geometry was prepared in CATIA 5 and convert into .igs file
- The geometry was imported to gambit for meshing process.
- Boundary conditions (inlet, outlet and wall) were applied.
- Material was assigned to the meshed part.
- The meshed part was saved and was exported into mesh file to be read in fluent software

- Mesh file was imported into FLUENT software.
- Grid checking was done to list the minimum and maximum x, y and z values from the grid in the default SI unit of meters.
- Next, grid scaling was done to set a unit to be mm for the whole process.
- Then, define model solver, viscosity, energy equation, material and initial condition for each boundary were assigned.
- Initialized the solver to be computed from the inlet towards the outlet of the blade.
- Enabled the plotting of residuals during the calculation by solving the residual monitor in order to monitor and determine the convergence criteria set in the monitor panel.
- Finally, the calculation was started by requesting 500 iterations.

- The results and interpretation of the predicted flow data.
- The main outcomes of post-processing are domain geometry and grid display, contour plot, vector plots, 2D surface plots, x-y plot with different properties and plot convergence

Figure 9: Summary of methodology for the whole simulation process

CHAPTER 4

RESULTS AND DISCUSSION

The simulation of the 2-D divergent blade began with simulation of a simplest geometry with only 1-D divergent. The work starts with the simplest case using a set of blades with only varying cross section, followed by the simulation of blades with only varying path length as shown in a table below:-

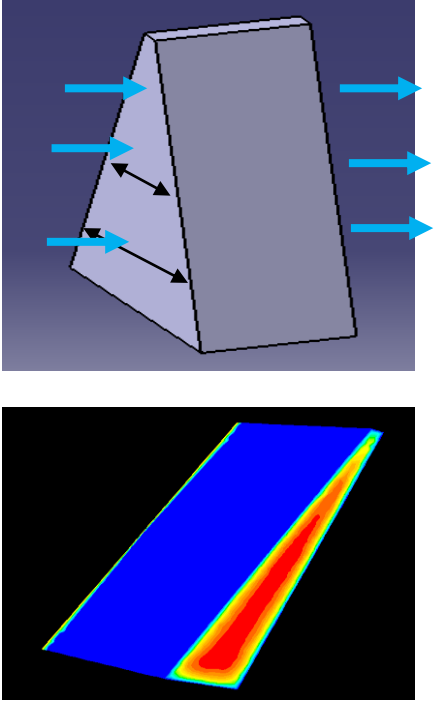
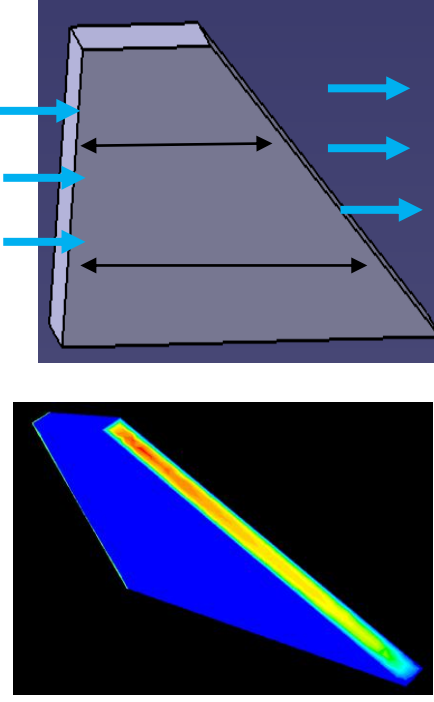
Divergent blade passage – varying cross section	Divergent blade passage – varying path length
 <p data-bbox="220 1451 699 1704">-The set of blades diverges along the direction of flow. Therefore, the air flows through the blade passage at various cross section areas from inlet to the outlet</p> <p data-bbox="220 1753 699 1951">-Larger cross section provides least resistance. Therefore, air tends to flow and is concentrated at the largest cross section at the outlet.</p>	 <p data-bbox="802 1451 1241 1704">-The set of blades diverges along the path length. Therefore, the air flows through the blade passage at various distances from inlet to the outlet.</p> <p data-bbox="802 1753 1241 1951">-Shorter distance provides least resistance. Therefore, air tends to flow and concentrated at the shortest path length at the outlet.</p>

Table 1: Simplest case for 1-D divergent blade passage

2-D divergent blade passage

Table below shows the overall analysis total of 128 cases with annular blade having various parameters including:-

- 1) 4 blade overlap angle - (9° , 12° , 15° , 18°)
- 2) 2 blade inclination angle - (15° to 20°)
- 3) 2 blade gaps - (3mm to 2mm) & (2mm to 1mm)
- 4) 2 blade types – short blade and long blade
- 5) 4 inlet velocities – 1.7m/s, 2.5m/s, 3.0m/s, 3.5m/s

Blade size		9 deg blade		12 deg blade		15 deg blade		18 deg blade	
Blade condition/blade gaps		(3 to 2) mm	(2 to 1) mm	(3 to 2) mm	(2 to 1) mm	(3 to 2) mm	(2 to 1) mm	(3 to 2) mm	(2 to 1) mm
normal size	velocities for 15 angle blade inclination	1.7 m/s	1.7 m/s	1.7 m/s	1.7 m/s	1.7 m/s	1.7 m/s	1.7 m/s	1.7 m/s
		2.5 m/s	2.5 m/s	2.5 m/s	2.5 m/s	2.5 m/s	2.5 m/s	2.5 m/s	2.5 m/s
		3.0 m/s	3.0 m/s	3.0 m/s	3.0 m/s	3.0 m/s	3.0 m/s	3.0 m/s	3.0 m/s
		3.5 m/s	3.5 m/s	3.5 m/s	3.5 m/s	3.5 m/s	3.5 m/s	3.5 m/s	3.5 m/s
Symmetry condition		1.7 m/s	1.7 m/s	1.7 m/s	1.7 m/s	1.7 m/s	1.7 m/s	1.7 m/s	1.7 m/s
		2.5 m/s	2.5 m/s	2.5 m/s	2.5 m/s	2.5 m/s	2.5 m/s	2.5 m/s	2.5 m/s
		3.0 m/s	3.0 m/s	3.0 m/s	3.0 m/s	3.0 m/s	3.0 m/s	3.0 m/s	3.0 m/s
		3.5 m/s	3.5 m/s	3.5 m/s	3.5 m/s	3.5 m/s	3.5 m/s	3.5 m/s	3.5 m/s
normal size	velocities for 20 angle blade inclination	1.7 m/s	1.7 m/s	1.7 m/s	1.7 m/s	1.7 m/s	1.7 m/s	1.7 m/s	1.7 m/s
		2.5 m/s	2.5 m/s	2.5 m/s	2.5 m/s	2.5 m/s	2.5 m/s	2.5 m/s	2.5 m/s
		3.0 m/s	3.0 m/s	3.0 m/s	3.0 m/s	3.0 m/s	3.0 m/s	3.0 m/s	3.0 m/s
		3.5 m/s	3.5 m/s	3.5 m/s	3.5 m/s	3.5 m/s	3.5 m/s	3.5 m/s	3.5 m/s
symmetry condition		1.7 m/s	1.7 m/s	1.7 m/s	1.7 m/s	1.7 m/s	1.7 m/s	1.7 m/s	1.7 m/s
		2.5 m/s	2.5 m/s	2.5 m/s	2.5 m/s	2.5 m/s	2.5 m/s	2.5 m/s	2.5 m/s
		3.0 m/s	3.0 m/s	3.0 m/s	3.0 m/s	3.0 m/s	3.0 m/s	3.0 m/s	3.0 m/s
		3.5 m/s	3.5 m/s	3.5 m/s	3.5 m/s	3.5 m/s	3.5 m/s	3.5 m/s	3.5 m/s

Table 2 : Analysis of SFB blade for 128 different cases

CALCULATIONS

However, before the simulations begin, some calculation has to be made to determine the reynold number in order to identify whether there is any possibility that the turbulent flow would occur.

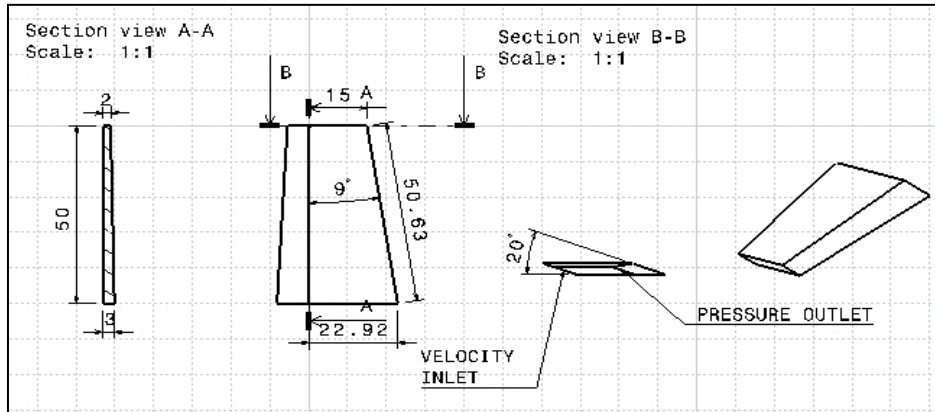
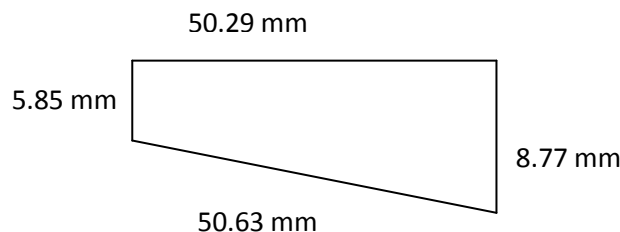


Figure 10 : Drafting of blade showing all the parameters for calculation.

Figure above shows one of the blade cases having 9° blade overlap angle, 20° blade inclination angle, and 2mm to 3mm blade gap. Based on the parameters shown, hydraulic number is calculated to determine Reynold number using formula :



$$\begin{aligned}
 Dh(\text{outlet}) &= \frac{4 \times \text{cross sec. area}(\text{trapezium})}{\text{wetted perimeter}} \\
 &= \frac{4 \times 0.5 \times (5.85 + 8.77)\text{mm} \times 50.63 \text{ mm}}{(115.54)\text{mm}} \\
 &= 12.81 \text{ mm}
 \end{aligned}$$

From the calculated hydraulic diameter, reynold number is determined using formula :

$$Re = VDh / \nu$$

Given ν = kinematic viscosity

$$= 1.6 \times 10^{-2} \text{ m}^2 / \text{s}$$

For the lowest velocity analyzed = 0.1 m/s,

$$\begin{aligned} \text{Re} &= \frac{0.1 \text{ m/s} \times 12.81 \text{ mm}}{1.6 \times 10^{-2} \text{ m}^2/\text{s}} \\ &= 80 \text{ (laminar flow)} \end{aligned}$$

For the highest velocity analyzed, = 3.5 m/s

$$\begin{aligned} \text{Re} &= \frac{3.5 \text{ m/s} \times 12.81 \text{ mm}}{1.6 \times 10^{-2} \text{ m}^2/\text{s}} \\ &= 2800 \text{ (slightly above laminar flow)} \end{aligned}$$

Reynolds number is a dimensionless number to measure the ratio between inertial force to viscous force. The value of Reynolds number is decided by the diameter and the velocity. Based on literature review, laminar flow is expected to occur at reynold number $\text{Re} < 2300$ while for turbulent is $\text{Re} > 4000$ for this case.

Based on the calculation above, the range for Reynold number $= 80 < \text{Re} < 2800$ and it is assumed that no turbulent flow is expected to occur within the blade passage.

SIMULATION

The purpose of having those 128 analyses is to validate whether or not the 5 factors mentioned above will affect the flow pattern through the short SFB blade. Some of the results are presented below :

Interpretation And Validation – for 9 degree blade overlap angle

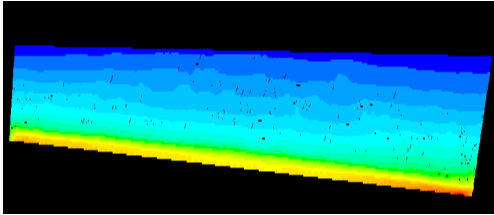
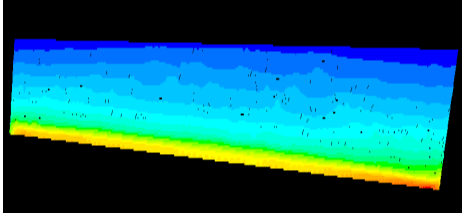
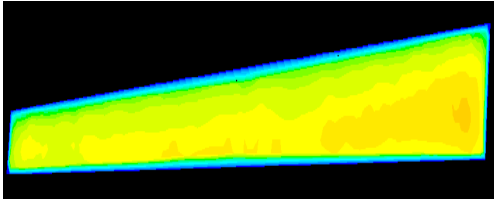
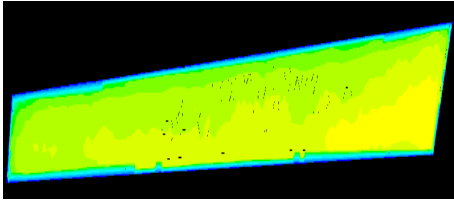
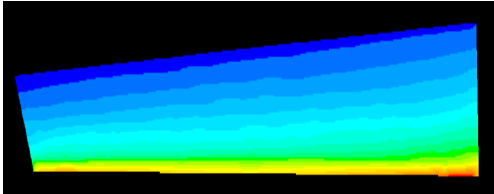
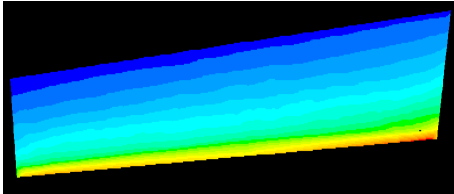
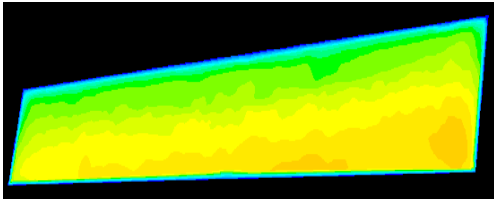
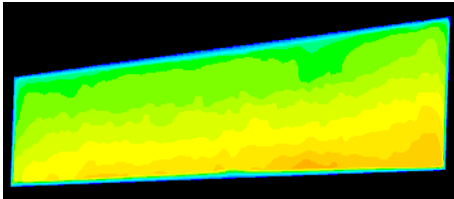
Variables	1.7 m/s	3.5 m/s
	15 angle inclination – 2mm to 1mm gap	
Pressure contour (inlet)		
Velocity contour (outlet)		
	15 angle inclination – 3mm to 2mm gap	
Pressure contour (inlet)		
Velocity contour (outlet)		

Table 3 : Velocity and pressure profile for 9 degree overlap angle with 15° inclination angle

Interpretation And Validation – for 9 degree blade overlap angle

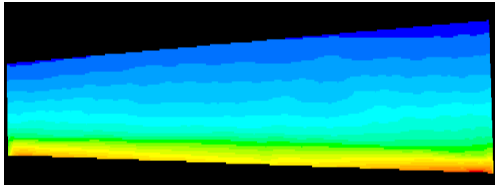
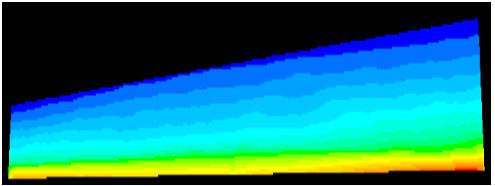
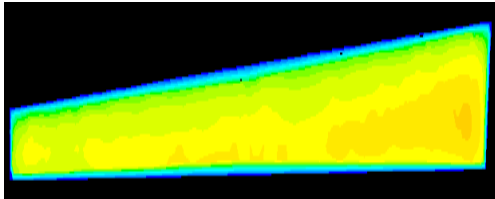
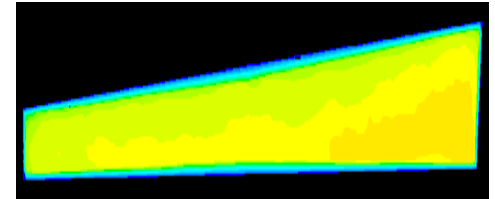
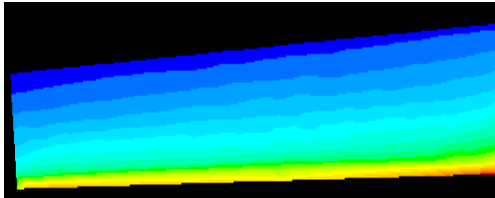
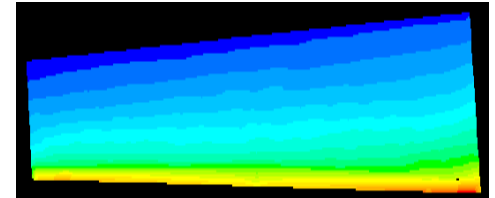
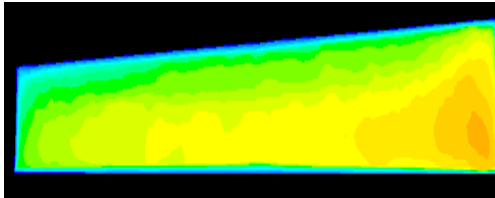
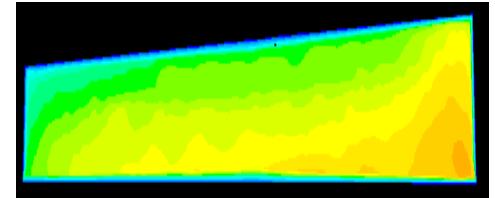
Variables	1.7 m/s	3.5 m/s
	20 angle inclination – 2mm to 1mm gap	
Pressure contour (inlet)		
Velocity contour (outlet)		
20 angle inclination – 3mm to 2mm gap		
Pressure contour (inlet)		
Velocity contour (outlet)		

Table 4 : Velocity and pressure profile for 9 degree overlap angle with 20° inclination angle

Interpretation And Validation – for 12 degree blade overlap angle

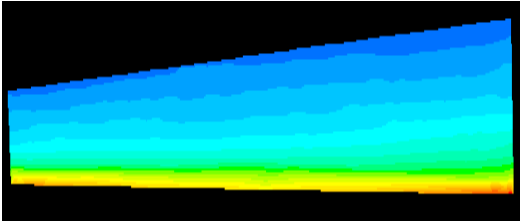
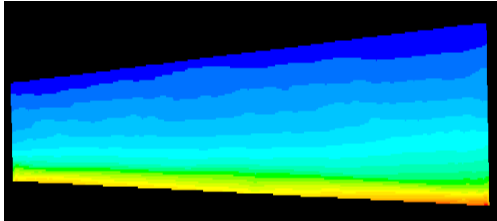
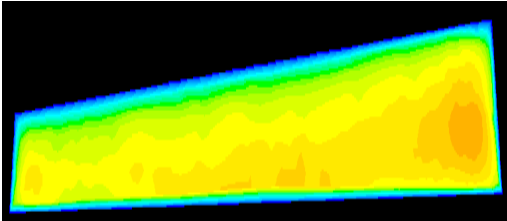
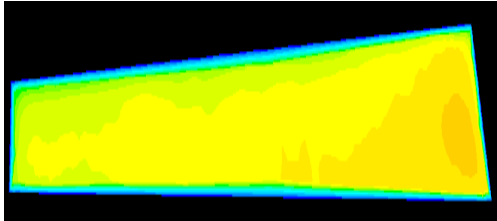
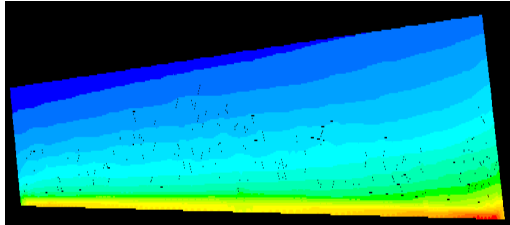
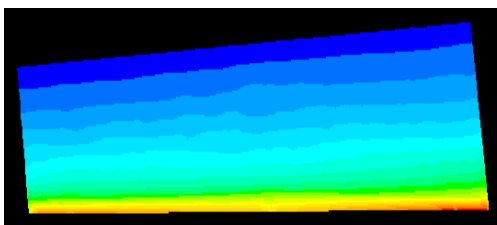
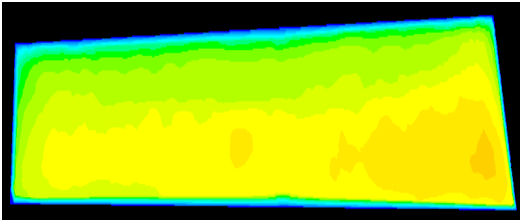
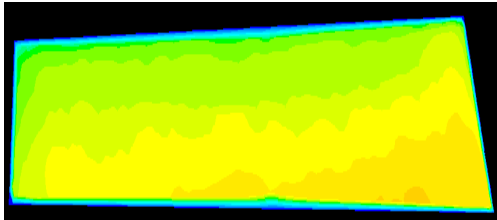
Variables	1.7 m/s	3.5 m/s
	15 angle inclination – 2mm to 1mm gap	
Pressure contour (inlet)		
Velocity contour (outlet)		
	15 angle inclination – 3mm to 2mm gap	
Pressure contour (inlet)		
Velocity contour (outlet)		

Table 5 : Velocity and pressure profile for 12 degree overlap angle with 15° inclination angle

Interpretation And Validation – for 12 degree blade overlap angle

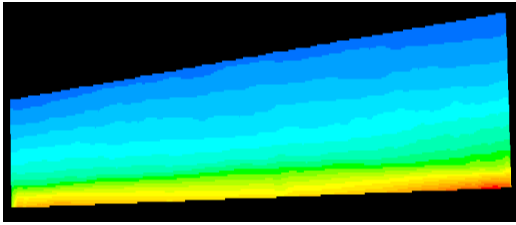
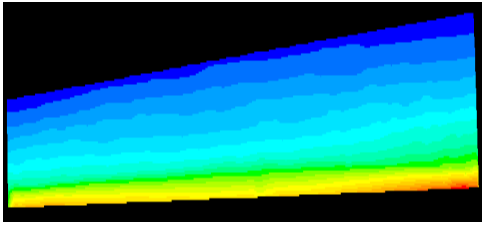
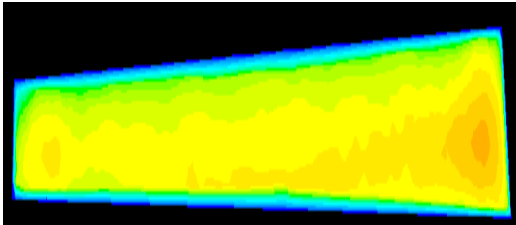
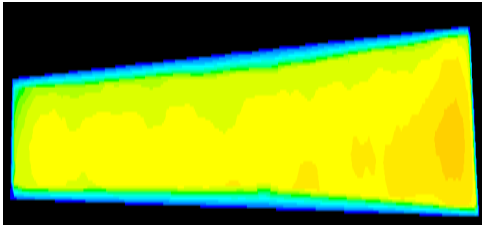
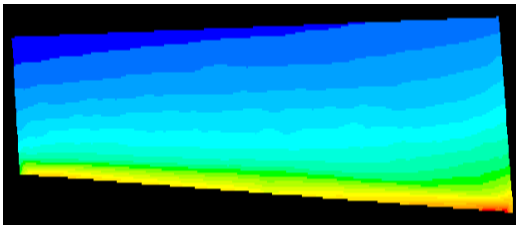
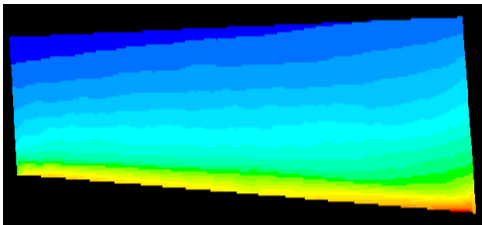
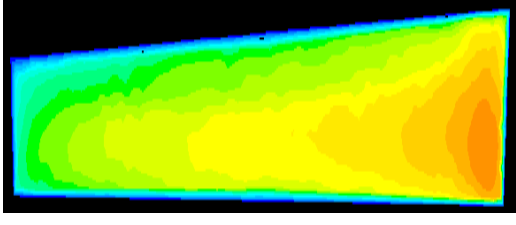
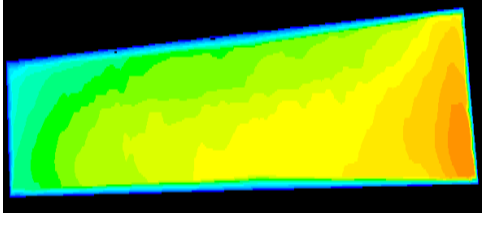
Variables	1.7 m/s	3.5 m/s
	20 angle inclination – 2mm to 1mm gap	
Pressure contour (inlet)		
Velocity contour (outlet)		
20 angle inclination – 3mm to 2mm gap		
Pressure contour (inlet)		
Velocity contour (outlet)		

Table 6 : Velocity and pressure profile for 12 degree overlap angle with 20° inclination angle

Based on some results presented above, only the magnitude of velocity is increasing with the increase of blade inclination and blade overlap angle. However, the flow patterns of both velocity and pressure profiles are same for all cases regardless the velocity variations, blade overlap angles etc. Therefore it can be said that all parameters has almost negligible effect on the flow characteristic within a short blade passage in SFB.

DISCUSSION

Based on Table 1, in the case of 1-D divergent blade passage with varying cross-section, it was observed that the fluid flowing from inlet through the blade passage is concentrated at the large cross section area at the outlet. This is because larger cross section provides least resistance to the flow. In the case of 1-D divergent blade passage with varying path length, the fluid flowing from inlet through the blade passage and concentrated at the outlet with the shortest path. This is because shorter path provides least resistance to the flow.

For the case of 2-D divergent blade passage, the small cross section (high resistance) was compensated with the short path (low resistance) while the large cross section area (low resistance) was compensated with a longer path (high resistance). The result shows that the fluid flow is concentrated at the outlet with a large cross section and longer path. It shows that the low resistance due to larger cross section area is more dominant than the shorter path length. Regardless of velocity variations at the inlet, the flow shows the similar pattern where the flow follows the path with least resistance.

Overall, the result shows when the inlet blade is inclined, it shows that the flow is concentrated at the bottom following the shortest path which determines that the boundary layer is asymmetric as shown in figure below.

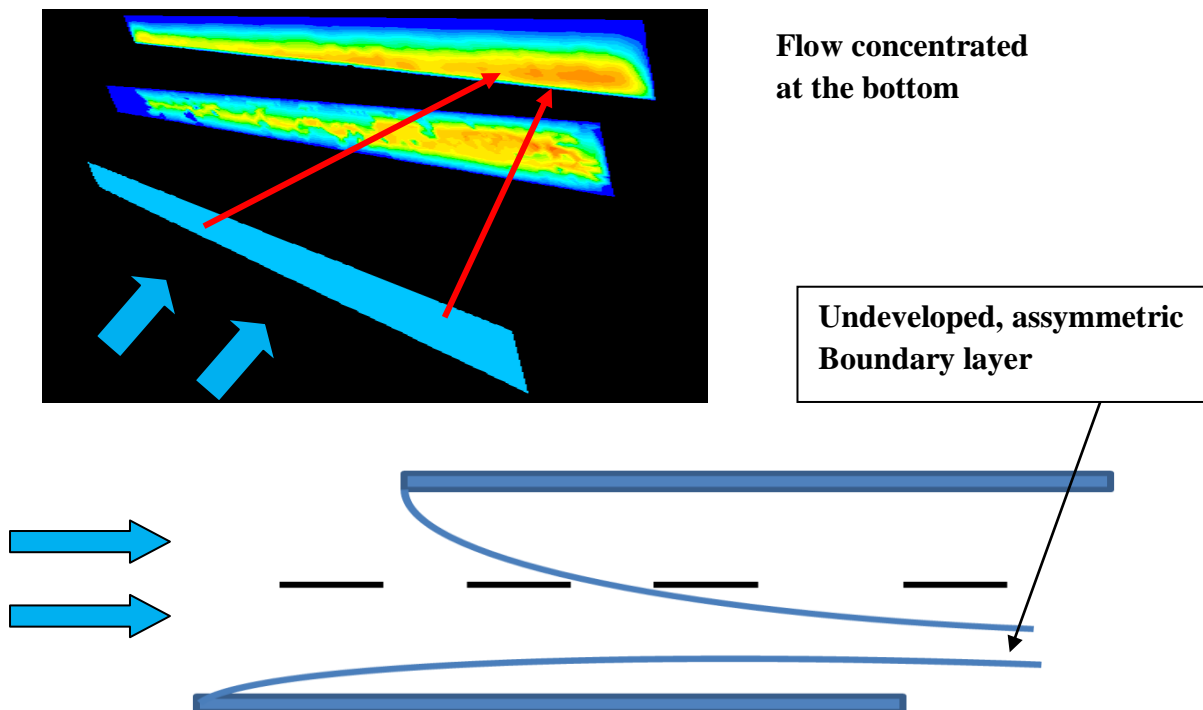


Figure 11 : Flow pattern and flow development in 2-D divergent blade passage

CHAPTER 5

CONCLUSIONS AND RECOMMENDATION

All objectives aimed at the beginning of the project are achieved which is to obtain the pressure and velocity variation at the distributor outlet of 2-D divergent trapezoidal blade based on various operating variables including air inlet velocity, geometry of cross-sections and blade length and blade width. This work also aims to get the flow variation if the blade opening is inclined.

In conclusion, the fluid tends to flow through the path with the least resistance which is having either the largest cross section area or the shortest distance between two blades. Comparing those factors, from the results it is seen that the low resistance due to larger cross section area is more dominant than the shorter path length. This is based on the case of 2-D divergent blade passage where the medium tends to flow at larger cross section even with the longer distance. Several simulations using different size of blade with various inlet velocities has been done to validate that the size of blade of inlet velocity has negligible impact on the flow variation between 2 blades.

It is recommended for further study with a curved set of blades as an annular distributor for swirling fluidized bed. Detail study on a long blade also can be done to compare with the current work on a short blade. More complex cases also can be simulated in further such as for the case of yaw flow where the flow entering the blade at the direction normal to the blade. The continuation of the current simulation for both the pressure and velocity specified at the blade inlet is also highly recommended.

CHAPTER 6

REFERENCES

- [1] N. Damean, and P.P.L. Regtien, (2001). Poiseuille number for the fully developed laminar flow through hexagonal ducts etched in $\langle 1\ 0\ 0 \rangle$ silicon. *Sensors and Actuators, A: Physical*, 90(1-2), 96-101.
- [2] S. K. Thomas, R. C. Lykins and K. L. Yerkes, Fully developed laminar flow in trapezoidal grooves with shear stress at the liquid–vapor interface *International Journal of Heat and Mass Transfer*, Volume 44, Issue 18, September 2001, 3397-3412
- [3] A. Husain and K. Y. Kim, Thermal Optimization of a Microchannel Heat Sink With Trapezoidal Cross Section *J. Electron. Packag.* 131, 021005 (2009)
- [4] J.P McHale. Garimella S.V. Heat transfer in trapezoidal microchannels of various aspect ratios (2010) , *International Journal of Heat and Mass Transfer*, 53 (1-3), pp. 365-375.
- [5] O. A. Huzayyin, R. M. Manglik, and M. A. Jog, Extended Results for Fully Developed Laminar Forced Convection Heat Transfer in Trapezoidal Channels of Plate-Fin Exchangers *J. Thermal Sci. Eng. Appl.* 2, 044501 (2010).
- [6] O. A. Huzayyin, R. M. Manglik, Computational modeling of convective heat transfer in converging-diverging plate channels with fin-wall perforation (2010) *ASME International Mechanical Engineering Congress and Exposition, Proceedings*, 9 (PART B), pp. 1173-1181.
- [7] N. Hilal, The relationship between particle properties and fluidizing velocity during fluidized bed heat transfer. *Advanced Powder Technology*, 15 5 (2004), pp. 583–594.
- [8] H.Z. Sheng, Heat-transfer study of external superheater of CFB incinerator. *Environmental Engineering Science*, 21 1 (2004), pp. 39–44.

- [9] L. Zhao, Drying of a dilute suspension in a revolving flow fluidized bed of inert particles. *Drying Technology*, 22 1–2 (2004), pp. 363–376.
- [10] B. Sreenivasan, and V.R. Raghavan (2000). “Hydrodynamics of a swirling fluidized bed”, Elsevier. Vol. 41. 99-106.
- [11] M. Kamil, M. Yusoff and V. R. Raghavan (2005) “Swirling Fluidized Beds - an advanced hydrodynamic model”. 4th International Conference on Heat Transfer, HEFAT, 4th Int. Conf. on Heat Transfer, Fluid Mechanics and Thermodynamics, Cairo, Egypt, Sept. 2005.
- [12] K. Dutkowski, Experimental investigations of Poiseuille number laminar flow of water and air in minichannels , *International Journal of Heat and Mass Transfer* Volume 51, Issues 25-26, December 2008, Pages 5983-5990.
- [13] M. Akbari, D. Sinton and M. Bahrami, Viscous flow in variable cross-section microchannels of arbitrary shapes , *International Journal of Heat and Mass Transfer*, Volume 54, Issues 17-18, August 2011, Pages 3970-3978
- [14] H. Niazmand, R. Metin and S. Ehsan, Developing slip-flow and heat transfer in trapezoidal microchannels, *International Journal of Heat and Mass Transfer* Volume 51, Issues 25-26, December 2008, Pages 6126-6135

CHAPTER 7

APPENDICES

Figure A1 : Defined solver

The image shows a software dialog box titled "Defined solver". It contains several groups of radio button options for configuring a solver. The groups are: "Solver" with "Segregated" (selected) and "Coupled"; "Formulation" with "Implicit" (selected) and "Explicit"; "Space" with "2D", "Axisymmetric", "Axisymmetric Swirl", and "3D" (selected); "Time" with "Steady" (selected) and "Unsteady"; "Velocity Formulation" with "Absolute" (selected) and "Relative"; "Gradient Option" with "Cell-Based" (selected) and "Node-Based"; and "Porous Formulation" with "Superficial Velocity" (selected) and "Physical Velocity". At the bottom are three buttons: "OK", "Cancel", and "Help".

Section	Options
Solver	<input checked="" type="radio"/> Segregated <input type="radio"/> Coupled
Formulation	<input checked="" type="radio"/> Implicit <input type="radio"/> Explicit
Space	<input type="radio"/> 2D <input type="radio"/> Axisymmetric <input type="radio"/> Axisymmetric Swirl <input checked="" type="radio"/> 3D
Time	<input checked="" type="radio"/> Steady <input type="radio"/> Unsteady
Velocity Formulation	<input checked="" type="radio"/> Absolute <input type="radio"/> Relative
Gradient Option	<input checked="" type="radio"/> Cell-Based <input type="radio"/> Node-Based
Porous Formulation	<input checked="" type="radio"/> Superficial Velocity <input type="radio"/> Physical Velocity

OK Cancel Help

Figure A2 : Defined material in FLUENT

Name	Material Type	Order Materials By
air	fluid	<input checked="" type="radio"/> Name <input type="radio"/> Chemical Formula
Chemical Formula	Fluent Fluid Materials	Fluent Database...
	air	User-Defined Database...
	Mixture	
	none	
Properties		
Density (kg/m³)	ideal-gas	Edit...
Cp (J/kg-K)	constant	Edit...
	1006.43	
Thermal Conductivity (W/m-K)	constant	Edit...
	0.0242	
Viscosity (kg/m-s)	constant	Edit...
	3.9e-05	
Change/Create Delete Close Help		

Figure A3 : Setup of velocity inlet in FLUENT

Zone Name	
<input type="text" value="inlet"/>	
Velocity Specification Method	<input type="text" value="Components"/>
Reference Frame	<input type="text" value="Absolute"/>
Coordinate System	<input type="text" value="Cartesian [X, Y, Z]"/>
X-Velocity (m/s)	<input type="text" value="0"/> <input type="text" value="constant"/>
Y-Velocity (m/s)	<input type="text" value="0"/> <input type="text" value="constant"/>
Z-Velocity (m/s)	<input type="text" value="1.7"/> <input type="text" value="constant"/>
Temperature (k)	<input type="text" value="300"/> <input type="text" value="constant"/>
Turbulence Specification Method	<input type="text" value="Intensity and Hydraulic Diameter"/>
Turbulence Intensity (%)	<input type="text" value="5"/>
Hydraulic Diameter (in)	<input type="text" value="39.37008"/>
<input type="button" value="OK"/> <input type="button" value="Cancel"/> <input type="button" value="Help"/>	

Figure A4 : setup of pressure outlet in FLUENT

The image shows the 'Pressure Outlet' setup dialog box in FLUENT. The 'Zone Name' is 'pressure_outlet'. The 'Gauge Pressure (pascal)' is set to 0, with a dropdown menu set to 'constant'. The 'Radial Equilibrium Pressure Distribution' checkbox is unchecked. The 'Backflow Total Temperature (K)' is set to 300, with a dropdown menu set to 'constant'. The 'Backflow Direction Specification Method' is set to 'Normal to Boundary'. The 'Turbulence Specification Method' is set to 'Intensity and Hydraulic Diameter'. The 'Backflow Turbulence Intensity (%)' is set to 5. The 'Backflow Hydraulic Diameter (in)' is set to 39.37008. The 'Target mass-flow rate' checkbox is unchecked. At the bottom are 'OK', 'Cancel', and 'Help' buttons.

Zone Name
pressure_outlet

Gauge Pressure (pascal) 0 constant

☐ Radial Equilibrium Pressure Distribution

Backflow Total Temperature (K) 300 constant

Backflow Direction Specification Method Normal to Boundary

Turbulence Specification Method Intensity and Hydraulic Diameter

Backflow Turbulence Intensity (%) 5

Backflow Hydraulic Diameter (in) 39.37008

☐ Target mass-flow rate

OK Cancel Help

Figure A5 : Graph of convergence

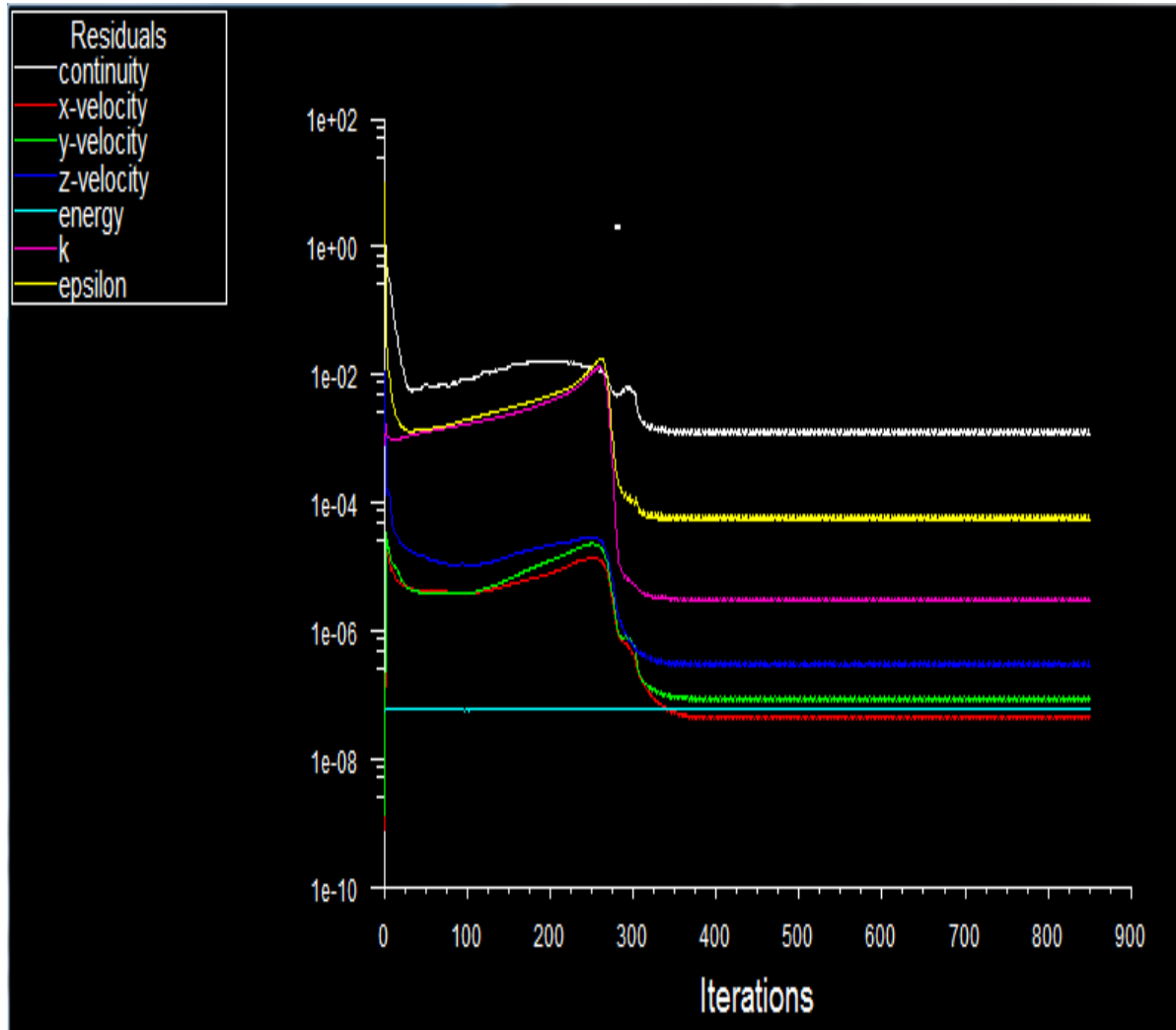


Table A1 : Interpretation And Validation – for 15° blade overlap angle

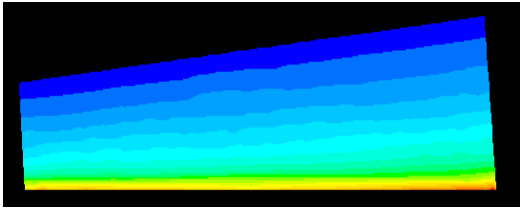
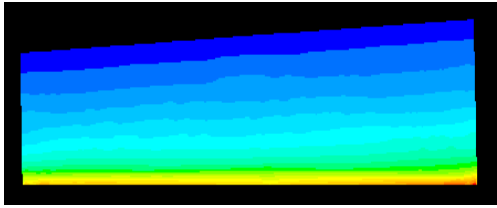
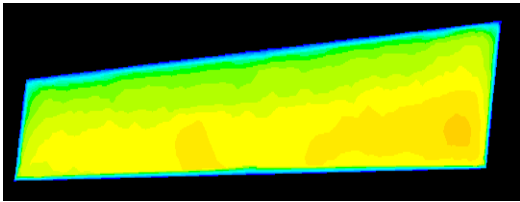
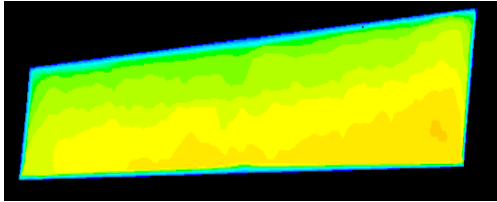
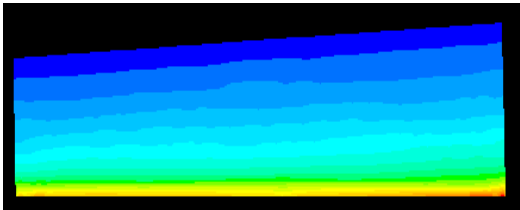
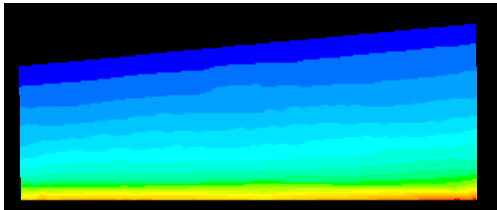
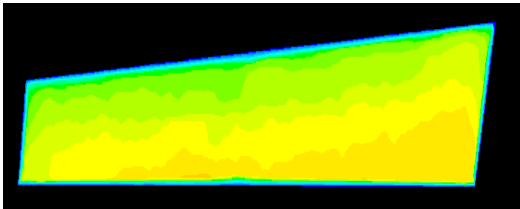
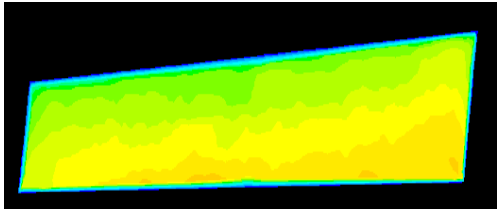
Variables	1.7 m/s	3.5 m/s
	15 angle inclination – 2mm to 1mm gap	
Pressure contour (inlet)		
Velocity contour (outlet)		
15 angle inclination – 3mm to 2mm gap		
Pressure contour (inlet)		
Velocity contour (outlet)		

Table A2 : Interpretation And Validation – for 15° blade overlap angle

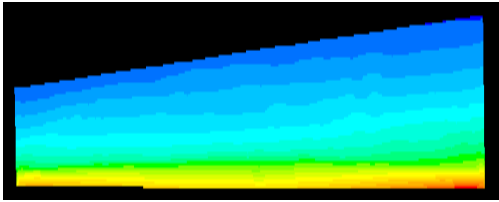
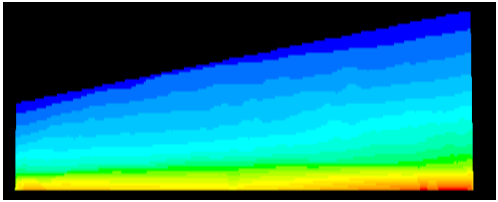
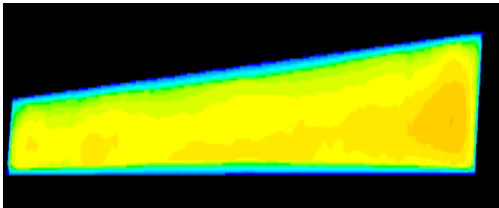
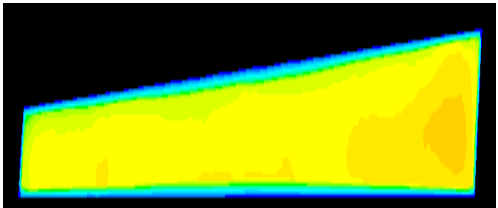
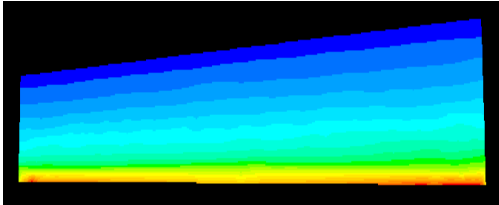
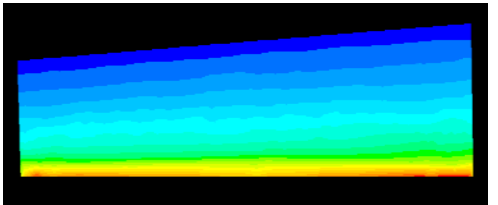
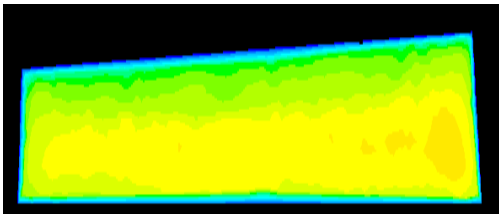
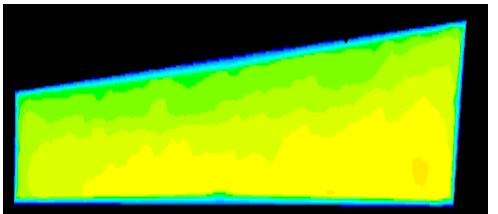
Variables	1.7 m/s	3.5 m/s
	20 angle inclination – 2mm to 1mm gap	
Pressure contour (inlet)		
Velocity contour (outlet)		
	20 angle inclination – 3mm to 2mm gap	
Pressure contour (inlet)		
Velocity contour (outlet)		

Table A3 : Interpretation And Validation – for 18° blade overlap angle

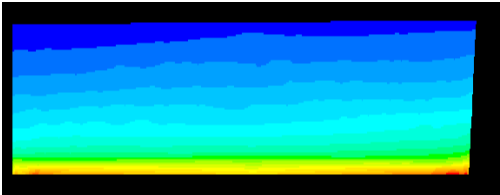
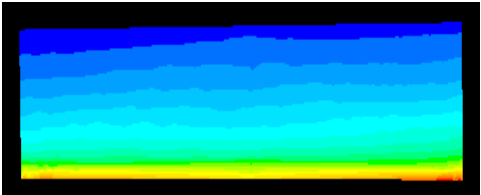
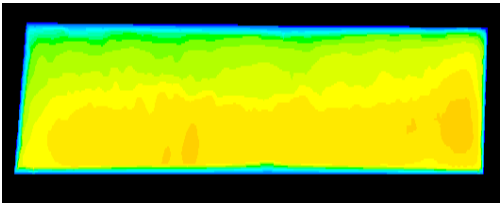
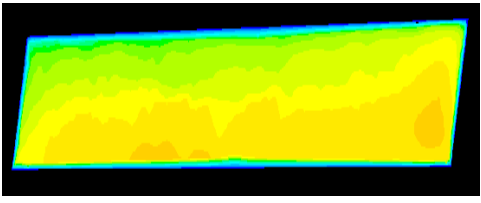
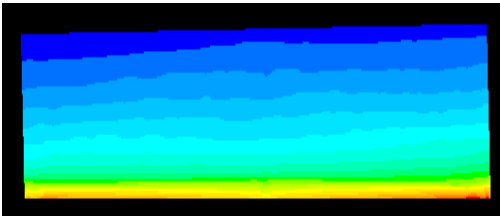
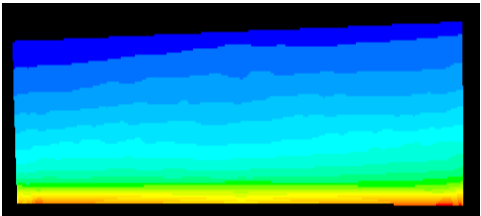
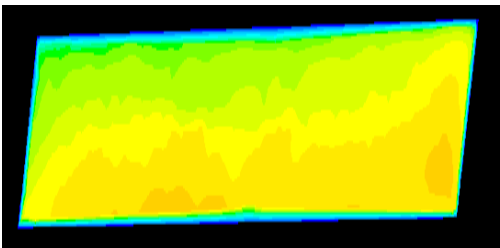
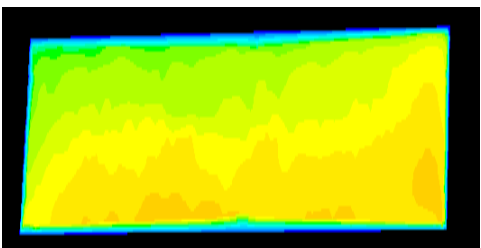
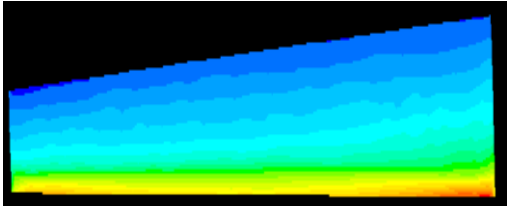
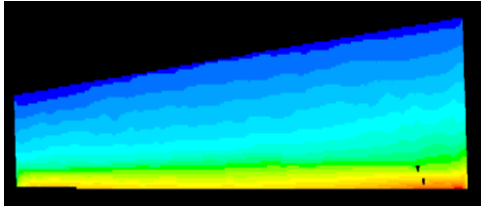
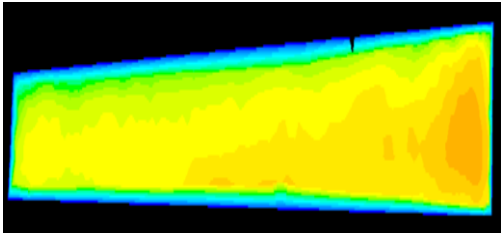
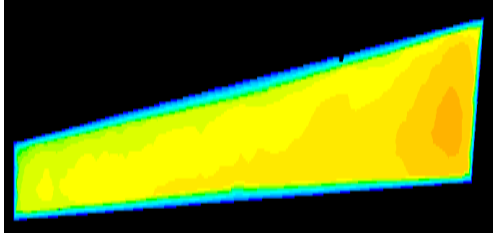
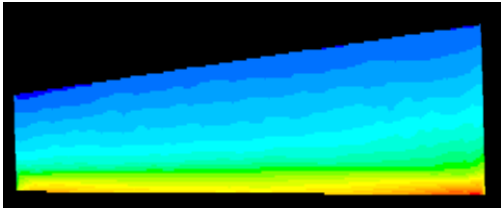
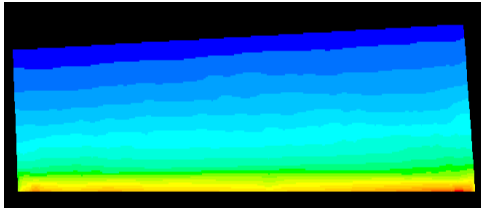
Variables	1.7 m/s	3.5 m/s
	15 angle inclination – 2mm to 1mm gap	
Pressure contour (inlet)		
Velocity contour (outlet)		
	15 angle inclination – 3mm to 2mm gap	
Pressure contour (inlet)		
Velocity contour (outlet)		

Table A4 : Interpretation And Validation – for 18° blade overlap angle

Variables	1.7 m/s	3.5 m/s
	15 angle inclination – 2mm to 1mm gap	
Pressure contour (inlet)		
Velocity contour (outlet)		
15 angle inclination – 3mm to 2mm gap		
Pressure contour (inlet)		
Velocity contour (outlet)	